Dilepton production by bremsstrahlung of meson fields in nuclear collisions

I.N. Mishustin[a,b], **L.M. Satarov**[a], **H. Stöcker**[c] **and W. Greiner**[c]

[a] *The Kurchatov Institute, 123182 Moscow, Russia*

[b] *The Niels Bohr Institute, DK–2100 Copenhagen Ø, Denmark*

[c] *Institut für Theoretische Physik, J.W. Goethe Universität, D–60054 Frankfurt am Main, Germany*

Abstract

We study the bremsstrahlung of virtual ω–mesons due to the collective deceleration of nuclei at the initial stage of an ultrarelativistic heavy–ion collision. It is shown that electromagnetic decays of these mesons may give an important contribution to the observed yields of dileptons. Mass spectra of e^+e^- and $\mu^+\mu^-$ pairs produced in central Au+Au collisions are calculated under some simplifying assumptions on the space–time variation of the baryonic current in a nuclear collision process. Comparison with the CERES data for 160 AGev Pb+Au collisions shows that the proposed mechanism gives a noticeable fraction of the observed e^+e^- pairs in the intermediate region of invariant masses. Sensitivity of the dilepton yield to the in–medium modification of masses and widths of vector mesons is demonstrated.

According to the relativistic mean–field model [1], strong time–dependent meson fields are generated in the course of a relativistic heavy–ion collision. Using the approach developed in papers on the pion [2] and photon [3] bremsstrahlung we suggested recently [4] a new mechanism of particle production by the collective bremsstrahlung and decay of classical meson fields in relativistic heavy–ion collisions. The comparison with the observed data on pion multiplicity shows [5] that this mechanism may be important in central collisions of most heavy nuclei already at the SPS bombarding energy.

Within this mechanism the production of some particle(s) i is considered as a two–step process $A_p + A_t \to \omega^* \to i + X$. Here $A_p(A_t)$ stands for the projectile (target) nucleus and ω^* is a virtual vector meson [1]. The first step in the above reaction corresponds to the virtual bremsstrahlung process leading to the creation of an off–mass–shell vector meson. The second step is the superposition of all channels of the virtual meson decay with the particle i in the final state. Below we consider the production of virtual mesons in the coherent process caused by the collective deceleration of the projectile and target nuclei at the initial stage of the reaction.

[1] Here and below the virtual particles (ω and γ) are marked by a superscript '$*$'.

Preliminary results concerning the contribution of the above mechanism to the production of pions, real ω–mesons and dileptons are published in Ref. [5].

Below we focus mainly on the dilepton emission in central collisions of ultrarelativistic nuclei. The analysis of the dilepton production is interesting at least by two reasons. First, dileptons are highly penetrating particles and carry practically an undistorted information about their creation points. Second, a strong enhancement of the dilepton yield was observed recently in central 200 AGeV S+Au [6], S+W [7] and 160 AGeV Pb+Au [8] collisions. The analysis shows [9–11] that this enhancement can only partially be explained by the conventional mechanism of binary hadron collisions, e.g. by $\pi\pi \to \rho \to e^+e^-$ processes. According to Refs. [9, 10] the experimental data can be reproduced assuming a strong reduction of the ρ meson mass in dense and hot nuclear matter. On the other hand, as argued in Ref. [11], the in–medium effect was probably overestimated in these calculations. Below we show that the enhanced dilepton yield may be explained, at least partly, by the contribution of the collective bremsstrahlung mechanism.

1. Formulation of the model

By analogy to the Walecka model we introduce the vector meson field $\omega^\mu(x)$ coupled to the 4–current $J^\mu(x)$ of baryons participating in a heavy–ion collision at a given impact parameter b. The equation of motion determining the space–time behaviour of $\omega^\mu(x)$ can be written as ($c = \hbar = 1$)

$$(\partial^\nu \partial_\nu + m_\omega^2)\,\omega^\mu(x) = g_V\,J^\mu(x)\,, \tag{1}$$

where g_V is the ωNN coupling constant and $m_\omega \simeq 783$ MeV is the omega meson mass. In the mean–field approximation ω^μ is considered as a purely classical field. From Eq. (1) one can see that excitation of propagating waves in the vacuum (the bremsstrahlung process) is possible if the Fourier transformed baryonic current

$$J^\mu(p) = \int \mathrm{d}^4x J^\mu(x) e^{ipx} \tag{2}$$

is nonzero in the time–like region $p^2 \sim m_\omega^2$.

In the following we study the bremsstrahlung process in the lowest order approximation neglecting the back reaction and reabsorption of the emitted vector mesons, i.e. treating J^μ as an external current. From Eq. (1) one can calculate the energy flux of the vector field at a large distance from the collision region [2]. Then this flux is expressed in terms of the distribution of field quanta, i.e. ω–mesons. This leads to the following formulae for the momentum distribution of real ω–mesons emitted in a heavy–ion collision [12]

$$E_\omega \frac{\mathrm{d}^3 N_\omega}{\mathrm{d}^3 p} = S(E_\omega, \boldsymbol{p})\,, \tag{3}$$

where $E_\omega = \sqrt{m_\omega^2 + \boldsymbol{p}^2}$ and

$$S(p) = \frac{g_V^2}{16\pi^3} |J_\mu^*(p) J^\mu(p)| \tag{4}$$

is a source function. In our model the latter is fully determined by the collective motion of the projectile and target nucleons.

To take into account the off–mass–shell effects we characterize virtual ω mesons by the mass $M_\omega \equiv \sqrt{p^2}$ and total width Γ_{ω^*}. The spectral function of virtual ω mesons may be written as

$$\rho(M_\omega) = \frac{2}{\pi} \frac{M_\omega \Gamma_{\omega^*}}{(M_\omega^2 - m_\omega^2)^2 + m_\omega^2 \Gamma_{\omega^*}^2}\,. \tag{5}$$

To calculate the distribution of virtual mesons in their 4–momenta p we use the formulae [5]

$$\frac{\mathrm{d}^4 N_{\omega^*}}{\mathrm{d}^4 p} = \rho(M_\omega) S(p)\,. \tag{6}$$

In the limit $\Gamma_{\omega^*} \to 0$ one can replace $\rho(M_\omega)$ by $2\delta(M_\omega^2 - m_\omega^2)$. In this case Eq. (6) becomes equivalent to the formulae (3) for the spectrum of the on–mass–shell vector mesons. Below we study also how the dilepton production is changed when the pole position in the vector meson propagator is shifted due to the medium effects.

We consider the following channels of the virtual ω decay, most important at invariant masses $M_\omega \lesssim m_\omega$: $i = e^+e^-$, $\mu^+\mu^-$, $\pi^0\gamma$, $\pi^0 e^+e^-$, $\pi^0\mu^+\mu^-$, $\pi^+\pi^-$, $\pi^+\pi^-\pi^0$. The total width Γ_{ω^*} is decomposed into the sum of partial decay widths $\Gamma_{\omega^* \to i}$:

$$\Gamma_{\omega^*} = \sum_i \Gamma_{\omega^* \to i}\,. \tag{7}$$

The distribution over the total 4–momentum of particles in a given decay channel can be written as

$$\frac{\mathrm{d}^4 N_{\omega^*\to i}}{\mathrm{d}^4 p} = B_{\omega^*\to i}\frac{\mathrm{d}^4 N_{\omega^*}}{\mathrm{d}^4 p}\,, \tag{8}$$

where $B_{\omega^*\to i} \equiv \Gamma_{\omega^*\to i}/\Gamma_{\omega^*}$ is the branching ratio of the i–th decay channel. The latter is a function of the total invariant mass of the decay particles $M = \sqrt{p^2} = M_\omega$.

To calculate the 4–current $J^\mu(p)$ determining the source function $S(p)$ we adopt the simple picture of a high–energy heavy–ion collision suggested in Ref. [4]. We consider collisions of identical nuclei ($A_p = A_t = A$) at zero impact parameter. In the equal velocity frame the projectile and target nuclei initially move towards each other with velocities $\pm v_0$ or rapidities $\pm y_0$, where $v_0 = \tanh y_0 = (1-4m_N^2/s)^{1/2}$ and $\sqrt{s}$ is the c.m. bombarding energy per nucleon. In the "frozen density" approximation [4] the internal compression and transverse motion of nuclear matter are disregarded at the early (interpenetration) stage of the reaction. Within this approximation the colliding nuclei move as a whole along the beam axis with instantaneous velocities $\dot{z}_p = -\dot{z}_t \equiv \dot{z}(t)$. The projectile velocity $\dot{z}(t)$ is a decreasing function of time, which we parametrize in the form [2]

$$\dot{z}(t) = v_f + \frac{v_0 - v_f}{1+\mathrm{e}^{t/\tau}}\,, \tag{9}$$

where τ is the effective deceleration time and v_f is the final velocity of nuclei (at $t \to +\infty$) .

In this approximation the Fourier transform of the baryon current $J^\mu(p)$ is totally determined by the projectile trajectory $z(t)$ [4]:

$$J^0(p) = \frac{p_\parallel}{p_0} J^3(p) = 2A\int\limits_{-\infty}^{\infty} \mathrm{d}t e^{ip_0 t}\cos\left[p_\parallel z(t)\right] F\left(\sqrt{\boldsymbol{p}_T^2 + p_\parallel^2\cdot[1-\dot{z}^2(t)]}\right)\,, \tag{10}$$

where $p_\parallel$ and $\boldsymbol{p}_T$ are, respectively, the longitudinal and transverse components of the three–momentum $\boldsymbol{p}$, $F(q)$ is the density form factor of the initial nuclei

$$F(q) \equiv \frac{1}{A}\int \mathrm{d}^3 r \rho(r) e^{-i\boldsymbol{q}\,\boldsymbol{r}} = \frac{4\pi}{Aq}\int\limits_0^\infty r\mathrm{d}r\rho(r)\sin qr\,. \tag{11}$$

The time integrals in Eq. (10) were calculated numerically assuming the Woods–Saxon distribution of the nuclear density $\rho(r)$.

In this work we choose the same coupling constant, g_V=13.78 and stopping parameters τ, v_f as in Ref. [4]. In particular, it is assumed that τ equals one half of the nuclear passage time

$$\tau = \frac{R}{\sinh y_0}\,, \tag{12}$$

where R is the geometrical radius of initial nuclei, $R = r_0 A^{1/3}$ with $r_0 = 1.12$ fm. Instead of v_f it is more convenient to introduce the c.m. rapidity loss δy defined by the relation:

$$v_f = \tanh\left(y_0 - \delta y\right). \tag{13}$$

For central Au+Au collisions we assume the energy–independent value [13] $\delta y = 2.4$ for $\sqrt{s} > 10$ GeV and the full stopping ($\delta y = y_0$) for lower bombarding energies.

2. Different channels of virtual meson decay and dilepton production

Similarly to Ref. [14] we assume that the "direct" decays of ω mesons into dileptons, $\omega^* \to l^+ l^-$, proceed via the intermediate emission and decay of virtual photons γ^*. In the following the explicit formulae are presented for the e^+e^- production only. The corresponding expressions for dimuons are obtained by replacing the lepton masses and decay widths. The matrix element of the process $\omega^* \to e^+e^-$ is proportional to the ω meson polarization vector ξ_μ, the lepton current $\overline{v}_+ \gamma^\mu u_-$ and the photon propagator k^{-2}, where $k = p_+ + p_-$ is the total 4–momentum of the lepton pair. The calculation of the partial decay width gives the result [14]

$$\Gamma_{\omega^* \to ee}(M) \propto M^{-3}\,\Gamma_{\gamma^* \to ee}\,. \tag{14}$$

Here $M = \sqrt{k^2}$ is the dilepton invariant mass (in the direct channel $M = M_\omega$) and $\Gamma_{\gamma^* \to ee}$ is the partial width of a virtual photon:

$$\Gamma_{\gamma^* \to ee} = \frac{\alpha\beta}{2}\left(1 - \frac{\beta^2}{3}\right)\Theta(M - 2m_e)\,, \tag{15}$$

where $\alpha = e^2/\hbar c$, $\Theta(x) \equiv \frac{1}{2}(1 + \mathrm{sign} x)$, m_e is the electron mass and

$$\beta = \sqrt{1 - \frac{4m_e^2}{M^2}}\,. \tag{16}$$

The proportionality coefficient in Eq. (14) is determined from the condition $B_{\omega^* \to ee}(m_\omega) = B_{ee}$ where $B_{ee} = 7.1 \cdot 10^{-5}$ is the observed probability of the $\omega \to ee$ decay [15].

We take into account also the three-particle, "Dalitz" decays $\omega^* \to \pi^0 e^+ e^-$. At fixed values of M and M_ω the components of the total dilepton 4-momentum k in the ω rest frame can be found by using the expressions

$$k_0 = \sqrt{\boldsymbol{k}^2 + M^2} = \frac{M^2 + M_\omega^2 - m_\pi^2}{2M_\omega}\,, \tag{17}$$

where $m_\pi = 0.14$ GeV is the pion mass. The corresponding partial width can be calculated assuming that the Dalitz decay is the two–step process $\omega^* \to \pi\gamma^* \to \pi ee$. Generalizing the results of [16] to the case of virtual ω's we obtain the following expression for the differential width of the Dalitz decay

$$\frac{\mathrm{d}\Gamma_{\omega^* \to \pi ee}}{\mathrm{d}M} = \frac{2}{\pi M^2} \Gamma_{\omega^* \to \pi\gamma^*} \Gamma_{\gamma^* \to ee}\,. \tag{18}$$

The $\omega^* \to \pi\gamma^*$ decay width is proportional to the electromagnetic form factor squared, $F_{\omega\pi}^2$:

$$\Gamma_{\omega^* \to \pi\gamma^*} \propto F_{\omega\pi}^2 |\boldsymbol{k}|^3 \Theta(M_\omega - M - m_\pi)\,, \tag{19}$$

where $|\boldsymbol{k}|$ is determined from Eq. (17). The coefficient of proportionality may be found by considering the limiting case $M_\omega \to m_\omega$, $M \to 0$, when the left hand side of Eq. (19) coincides with the observed width of the $\omega \to \pi\gamma$ decay. As shown in [16] the experimental data for $F_{\omega\pi}$ are well reproduced within the vector meson dominance model [17]. Assuming that this model is valid also for decays of virtual ω's we have

$$F_{\omega\pi}^2 = \frac{m_\rho^2\,(m_\rho^2 + \Gamma_\rho^2)}{(M^2 - m_\rho^2)^2 + m_\rho^2 \Gamma_\rho^2}\,, \tag{20}$$

where m_ρ and Γ_ρ are the mass and total width of the ρ meson. Unless otherwise stated, Eq. (20) is used with the parametrization $\Gamma_\rho = \Gamma_\rho(M)$ suggested in Ref. [14] and the free ρ meson mass ($m_\rho = m_{\rho 0} \simeq 0.77$ GeV).

To calculate the total width of virtual ω's one should also know the partial widths of non-electromagnetic decay channels. In the considered region of masses $M_\omega \lesssim 1$ GeV we take into account the decays with two and three pions in the final state. Assuming that the $\omega^* \to 2\pi$

matrix element is proportional to the product of the ω meson polarization vector and the difference of the pion 4–momenta, we get

$$\Gamma_{\omega^*\to 2\pi}(M_\omega) \propto M_\omega^{-2} \cdot \left(M_\omega^2 - 4m_\pi^2\right)^{3/2} \Theta(M_\omega - 2m_\pi)\,. \tag{21}$$

The proportionality coefficient is taken from the condition $B_{\omega^*\to 2\pi}(m_\omega) = B_{2\pi} = 0.022$ [15]. The $\omega^* \to 3\pi$ partial width is calculated assuming that it is proportional to the 3–pion phase space volume allowed by the kinematics [12]:

$$\Gamma_{\omega^*\to 3\pi}(M_\omega) \propto \Phi_{3\pi}(M_\omega) \cdot \Theta(M_\omega - 3m_\pi)\,, \tag{22}$$

with the coefficient determined from the relation $B_{\omega^*\to 3\pi}(m_\omega) = B_{3\pi} = 0.89$ [15].

The mass distribution of e^+e^- pairs produced by the bremsstrahlung mechanism can be written as a convolution of the virtual ω meson spectrum and the differential branching of the $\omega^* \to eeX$ decay (X denotes any particle(s) emitted together with the lepton pair):

$$\frac{\mathrm{d}N_{ee}}{\mathrm{d}M} = \int \mathrm{d}^4 p_\omega \frac{\mathrm{d}^4 N_{\omega*}}{\mathrm{d}^4 p_\omega} \cdot \frac{\mathrm{d}B_{\omega^*\to eeX}}{\mathrm{d}M}\,. \tag{23}$$

Taking into account only the direct and Dalitz decays, the dilepton mass distribution can be represented as:

$$\frac{\mathrm{d}N_{ee}}{\mathrm{d}M} = B_{\omega^*\to ee} \frac{\mathrm{d}N_{\omega_*}}{\mathrm{d}M} + \int\limits_{M+m_\pi}^{\infty} \mathrm{d}M_\omega \frac{\mathrm{d}N_{\omega_*}}{\mathrm{d}M_\omega} \cdot \frac{\mathrm{d}B_{\omega^*\to ee\pi}}{\mathrm{d}M}\,. \tag{24}$$

The first (direct) term is obtained by using the relation $\mathrm{d}B_{\omega^*\to ee}/\mathrm{d}M = B_{\omega^*\to ee}\delta(M - M_\omega)$ and performing the explicit integration over M_ω.

To compare the model predictions with experimental data one should take into account the various acceptance cuts used in different experiments. This severely complicates the calculations: in general one should know the differential branching $\mathrm{d}^6 B_{\omega^*\to eeX}/\mathrm{d}^3 p_+ \mathrm{d}^3 p_-$ which describes the probability of the ω meson decay into the lepton pair with the positron and electron 3–momenta $\boldsymbol{p}_+$ and $\boldsymbol{p}_-$, respectively. To calculate the acceptance weighted mass distribution one should replace $\mathrm{d}B_{\omega^*\to eeX}/\mathrm{d}M$ in Eq. (23) by

$$\frac{\mathrm{d}B^{(A)}_{\omega^*\to eeX}}{\mathrm{d}M} = \int \mathrm{d}^3 p_+ \mathrm{d}^3 p_-\, \mathcal{A} \cdot \frac{\mathrm{d}^6 B_{\omega^*\to eeX}}{\mathrm{d}^3 p_+ \mathrm{d}^3 p_-} \delta(M - \sqrt{k^2})\,. \tag{25}$$

The weight function $\mathcal{A}$ equals one (zero) if $\boldsymbol{p}_\pm$ are inside (outside) the kinematical volume covered in a given experiment. In numerical calculations presented in the next section we use for e^+e^- pairs the acceptance cuts of the CERES experiment [8]

$$p_{T\pm} > 0.175 \text{ GeV/c}, \; 2.1 < \eta_\pm < 2.65, \; \theta_{ee} > 0.035\,. \tag{26}$$

Here $p_{T\pm}$ and $\eta_\pm$ are the transverse momenta and pseudorapidities of leptons, θ_{ee} is their relative emission angle in the lab frame.

At given M and M_ω the components of the vectors $\boldsymbol{p}_\pm$ are fixed by the angular variables $\Omega = (\theta, \phi)$ and $\tilde{\Omega} = (\tilde{\theta}, \tilde{\phi})$, where Ω denotes spherical angles of $\boldsymbol{k}$ with respect to the ω meson 3–momentum (in its rest frame) and $\tilde{\Omega}$ stands for the positron emission angles with respect to $\boldsymbol{k}$ (in the pair rest frame). By using these variables one can rewrite Eq. (25) as follows

$$\frac{\mathrm{d}B^{(A)}_{\omega^*\to eeX}}{\mathrm{d}M} = \frac{\mathrm{d}B_{\omega^*\to eeX}}{\mathrm{d}M}\int \mathrm{d}\Omega \int \mathrm{d}\tilde{\Omega}\, \frac{\mathrm{d}W_{\omega^*\to eeX}}{\mathrm{d}\Omega \mathrm{d}\tilde{\Omega}}\,\mathcal{A}\,, \tag{27}$$

where $\mathrm{d}W_{\omega^*\to eeX}/\mathrm{d}\Omega\mathrm{d}\tilde{\Omega}$ is the angular distribution of the $\omega^* \to eeX$ decay normalized to unity.

In our case the usual procedure of calculating the direct and Dalitz parts of dilepton distributions by simple averaging over all polarizations of decaying ω mesons is not correct. Indeed, as seen from Eq. (1), the polarization vector of a virtual vector meson ξ_μ is proportional to $J_\mu(p)$ where p is the meson 4–momentum. In the ω meson rest frame $\xi_\mu = (0, \boldsymbol{\xi})$, where $\boldsymbol{\xi}$ is a vector parallel to the direction of $\boldsymbol{p}$. Proceeding from the $\omega^* \to ee$ matrix element (see above) we get the following relation for the direct part of the angular distribution

$$\frac{\mathrm{d}W_{\omega^*\to ee}}{\mathrm{d}\Omega \mathrm{d}\tilde{\Omega}} = C_{\mathrm{dir}}\,\left(1 - \beta^2\cos^2\tilde{\theta}\right)\,\delta(\Omega)\,, \tag{28}$$

where C_{dir} is the normalization constant. The anisotropy of the lepton angular distribution in the rest frame of the ω meson is a consequence of its polarization.

The Dalitz part of the dilepton distribution is calculated assuming [14, 16] that the $\omega^* \to ee\pi$ matrix element is proportional to $\epsilon_{\mu\nu\sigma\delta}\xi^\mu p^\nu k^\sigma(\overline{v}_+\gamma^\delta u_-)$. The direct calculation gives

$$\frac{\mathrm{d}W_{\omega^*\to ee\pi}}{\mathrm{d}\Omega \mathrm{d}\tilde{\Omega}} = C_{\mathrm{dal}}\,\sin^2\theta\left[1 - \beta^2\sin^2\tilde{\theta}\,\sin^2(\tilde{\phi} - \phi)\right]\,, \tag{29}$$

where C_{dal} is found from the normalization condition. The averaging over the ω meson polarizations is equivalent to the averaging over Ω. As a result we obtain the distribution over $\tilde{\Omega}$ obtained earlier in Ref. [18].

3. Results

Let us now discuss the results of numerical calculations obtained within the model described above. One should bear in mind that the model assumes a rather simplified space—time evolution, in particular the collective projectile–target deceleration (see the discussion in Ref. [4]). Therefore, the model in its present form can be used for a qualitative analysis only.

Fig. 1 shows the dilepton mass spectrum in central ($b = 0$) 160 AGeV Au+Au collisions. One can see that the mass distribution of dileptons produced by the virtual ω decays is quite different from that predicted by the conventional hadronic sources. In particular, the low and intermediate mass region is strongly enhanced. This is explained by the copious production of "soft" virtual ω's by the bremsstrahlung mechanism. The contribution of direct ω decays is peaked at very small invariant masses as well as at the pole position of the ω propagator, $M = m_\omega$. The Dalitz contribution is most important in the intermediate region of dilepton masses, 0.2 GeV $\lesssim M \lesssim$ 0.6 GeV. A similar behaviour is predicted for the dimuon spectrum [2], Fig. 2. The main difference here is the much higher mass threshold at $M = 2m_\mu$.

In Fig. 3 we compare the model predictions for the same reaction, but at different bombarding energies, $\sqrt{s} = 17.43$ AGeV (SPS) and 200 AGeV (RHIC). We have also calculated the dilepton spectra at the LHC energy $\sqrt{s}$=6.3 ATeV but the corresponding results practically coincide with the model prediction for the RHIC energy. Such a behavior follows from the energy independence of the stopping parameter δy, assumed at high $\sqrt{s}$ (see Sect. 1). As a consequence, the phase–space distribution of primordial ω mesons, produced by the bremsstrahlung mechanism, saturates with raising bombarding energy [4].

The experimental acceptance cuts and a poor mass resolution distort significantly the dilepton mass distributions as compared to those presented in Figs. 1–3. In Fig. 4 we show the dilepton mass spectrum for central 160 AGeV Au+Au collisions. The CERES acceptance cuts and mass resolution are included in this calculation. The double differential spectrum $d^2N_{ee}/dMd\eta$ is obtained by dividing the acceptance weighted mass distribution, Eq. (24), by the width of the CERES pseudorapidity window. In calculating the acceptance weight $\mathcal{A}$ entering Eq. (27)

[2]Since the branching ratio of the direct decay $\omega \to \mu^+\mu^-$ is not known experimentally [15] we assume that it is equal to $B(\omega \to e^+e^-)$.

we have neglected the transverse momenta of primordial ω mesons (see Ref. [4]). At the same figure we show separately the contributions of direct and Dalitz decays of ω mesons. Note that the original spectrum (without mass resolution corrections) of e^+e^- pairs has a strong peak at $M \simeq m_\omega$. This peak originates from the direct ω meson decays. The step–like behaviour of the direct contribution at $M \simeq 0.35$ GeV appears due to the CERES cut at small transverse momenta, $p_{T\pm} > p_{\min}$=0.175 GeV/c. Indeed, in the limit $p_{T\omega} = 0$ the minimal invariant mass of "direct" pairs is $2\sqrt{m_e^2 + p_{\min}^2} \approx 0.35$ GeV. Taking into account nonzero components of $\boldsymbol{p}_{T\omega}$ will result in a certain smoothening of the above–mentioned jump in the dilepton mass distribution.

As one can see from Fig. 4, the bremsstrahlung mechanism gives a significant contribution to the dilepton production in the intermediate mass region. Hopefully, this contribution can be observed experimentally by using a characteristic angular distribution in the dilepton momentum predicted by the model [4, 5]. However, the bremsstrahlung contribution alone is not sufficient to explain the dilepton yield observed in central 160 AGeV Pb+Au collisions. In the most interesting region of masses $M \simeq 0.4 - 0.6$ GeV the data are underestimated by a factor of about three.

A special calculation showed that this discrepancy can not be removed by taking into account the excitation and decays of virtual ρ mesons disregarded in the present calculation. The contribution of the ρ meson bremsstrahlung in symmetric heavy–ion collisions is proportional to the isospin asymmetry factor $\chi = (1/2 - Z/A)^2$ where Z and A are the charge and mass numbers of the colliding nuclei. Since $\chi \lesssim 10^{-2}$, the role of the ρ meson bremsstrahlung is relatively small even for heaviest nuclei.

Of course, in addition to the collective bremsstrahlung mechanism the usual, incoherent, sources of dilepton production (e.g. the $\pi\pi \to ee$ and $\pi \to ee\gamma$ processes) also give a noticeable contributions. According to Refs. [9–11] the dynamical models incorporating only these incoherent hadronic sources may easily explain the low mass dilepton yields in S+Au and Pb+Au collisions at the SPS energies. On the other hand, these models significantly underestimate the observed data in the intermediate mass region. As argued in Refs. [9, 10] the agreement with experimental data can be achieved if one assumes a strong reduction of the vector meson masses in dense nuclear matter.

To check the sensitivity of our model to the in–medium modification of the vector mesons, in Fig. 5 we compare the dilepton mass distributions calculated for different values of the ρ and ω masses. To diminish the number of model parameters we take the same mass reduction factor for ρ and ω mesons: $m_\rho/m_{\rho 0} = m_\omega/m_{\omega 0} \equiv R_m$. One can see that the dilepton mass distribution is rather sensitive to R_m. A relatively small, 20 %, reduction of the meson masses raises the dilepton yield at $M \sim 0.5$ GeV by a factor of about two. On the other hand, the model calculation with fixed R_m predicts too high peaks in mass distributions. One should bear in mind that these calculations provide only a rough estimate of the possible effect since in an actual nuclear collision mass shifts should be time (and space) dependent. Therefore, the observed distribution will be a superposition of contributions with different R_m. As a result, the peak of direct dileptons will be less pronounced in this distribution.

As calculations of Ref. [19] show, the ω meson width may be significantly increased in dense baryonic matter due to the mixing of σ and ω mesons [1]. At baryonic densities of about two times the normal nuclear density, the width may increase by a factor of about 5 as compared to its vacuum value. To estimate the effects of the in–medium broadening of virtual ω mesons, we have performed the calculation where the partial decay widths were scaled by the same amplification factor λ, independent of M_ω. The calculation shows that this broadening influences mainly the direct component of the dilepton yield. As seen from Fig. 6, the yield in the intermediate mass region may be strongly enhanced at $\lambda \gtrsim 5$.

4. Summary

In conclusion, we have shown that the collective bremsstrahlung of the vector meson field can provide an important source of dilepton production in high energy heavy–ion collisions. This mechanism may be responsible, at least partly, for the enhanced yield of dileptons observed in central nuclear collisions at the SPS bombarding energies. It has been demonstrated that the coherent dilepton production is sensitive to the in–medium modification of vector meson masses and widths. Obviously, these effects should be studied in more details in microscopic models.

In future studies one should implement a more realistic dynamical picture of a heavy–ion collision by using either the fluid–dynamical or kinetic approaches. In this way one can take into account the flow and compression effects disregarded in present model. Also the formalism should be generalized to study bremsstrahlung effects in a situation when masses and widths of vector mesons are space and time dependent. To extend the calculations to collider energies, $\sqrt{s} \geq 200$ GeV, the model should be reformulated at the quark–gluon level.

5. Acknowledgments

The authors thank J.P. Bondorf and L.A. Winckelmann for useful discussions, J. Stachel and Th. Ullrich for providing a valuable information on CERES data. This work has been supported in part by the Carlsberg Foundation (Denmark) and EU–INTAS Grant No. 94–3405. We acknowledge also the financial support from GSI, BMFT and DFG. Two of us (I.N.M., L.M.S.) thank the Institute for Theoretical Physics, University of Frankfurt am Main, and the Niels Bohr Institute, University of Copenhagen, for the kind hospitality and financial support.

References

[1] B.D. Serot and J.D. Walecka, Adv. in Nucl. Phys. **16**, 1 (1985).

[2] D. Vasak, H. Stöcker, B. Müller, and W. Greiner, Phys. Lett. **93B**, 243 (1980); D. Vasak, B. Müller, and W. Greiner, Phys. Scr. **22**, 25 (1980).

[3] T. Lippert, U. Becker, N. Grün, W. Scheid, and G. Soff, Phys. Lett. **B207**, 366 (1988).

[4] I.N. Mishustin, L.M. Satarov, H. Stöcker, and W. Greiner, Phys. Rev. C **52**, 3315 (1995).

[5] I.N. Mishustin, L.M. Satarov, and H. Stöcker, in Proc. Int. Conf. *Nuclear Physics at the Turn of the Millenium* (Wilderness, South Africa, 1996), eds. H. Stöcker, A. Gallman,

J.H. Hamilton, World Scientific, 1997, p. 522;
I.N. Mishustin, L.M. Satarov, H. Stöcker, and W. Greiner, Preprint hep–ph/9611295 (1996).

[6] G. Agakishiev et al. (CERES Collab.), Phys. Rev. Lett. **75**, 1272 (1995).

[7] M. Masera for the HELIOS–3 Collab., Nucl. Phys. **A590**, 93c (1995).

[8] G. Agakishiev et al. (CERES Collab.), Nucl. Phys. **A610**, 317c (1996).

[9] G.Q. Li, C.M. Ko, and G.E. Brown, Phys. Rev. Lett. **75**, 4007 (1995);
C.M. Ko, G.Q. Li, G.E. Brown, and H. Sorge, Nucl. Phys. **A610**, 342c (1996).

[10] W. Cassing, W. Ehehalt, and C.M. Ko, Phys. Lett. **B363**, 35 (1995).

[11] L.A. Winckelmann et al., Nucl. Phys. **A610**, 116c (1996).

[12] Yu.B. Ivanov, Nucl. Phys. **A495**, 633 (1989).

[13] Th. Schönfeld, H. Stöcker, W. Greiner and H. Sorge, Mod. Phys. Lett. A **8**, 2631 (1993).

[14] P. Koch, Z. Phys. C **57**, 283 (1993).

[15] Particle Data Group, Review of Particle Properties, Phys. Rev. D **50**, 1173 (1994).

[16] L.G. Landberg, Phys. Rep. **128**, 301 (1985).

[17] J.J. Sakurai, *Currents and Mesons* (University of Chicago Press, Chicago, 1969).

[18] N.M. Kroll and W. Wada, Phys. Rev. **98**, 1355 (1955).

[19] G. Wolf, B. Friman, and M. Soyer, GSI Report GSI–96–1 (Darmstadt, 1996), p. 70.

Figure captions

Fig. 1. Mass spectrum of e^+e^- pairs produced by the collective bremsstrahlung mechanism in central 160 AGeV Au+Au collisions. Contributions of the direct ($\omega_* \to ee$) and Dalitz ($\omega^* \to \pi ee$) decay channels are shown by dotted and dashed line respectively.

Fig. 2. The same as in Fig. 1, but for the spectrum of $\mu^+\mu^-$ pairs.

Fig. 3. Comparison of e^+e^- yields in central Au+Au collisions at the SPS and RHIC bombarding energies.

Fig. 4. Mass spectrum of e^+e^- pairs produced by the collective bremsstrahlung mechanism in central 160 AGeV Au+Au collisions. The grey histogram (solid line) shows the model results with (without) inclusion of experimental mass resolution. The dotted (dashed) line shows the contribution of direct (Dalitz) ω meson decays. Preliminary experimental data for central Pb+Au collisions [8] are shown by solid circles.

Fig. 5. Comparison of e^+e^- spectra in central 160 AGeV Au+Au collision for different values of the meson mass reduction factor R_m. Preliminary experimental data for central Pb+Au collisions are taken from Ref. [8].

Fig. 6. The same as in Fig. 5 but for different choices of the virtual ω width in units of the vacuum width $\Gamma_0 = 8.4$ MeV.

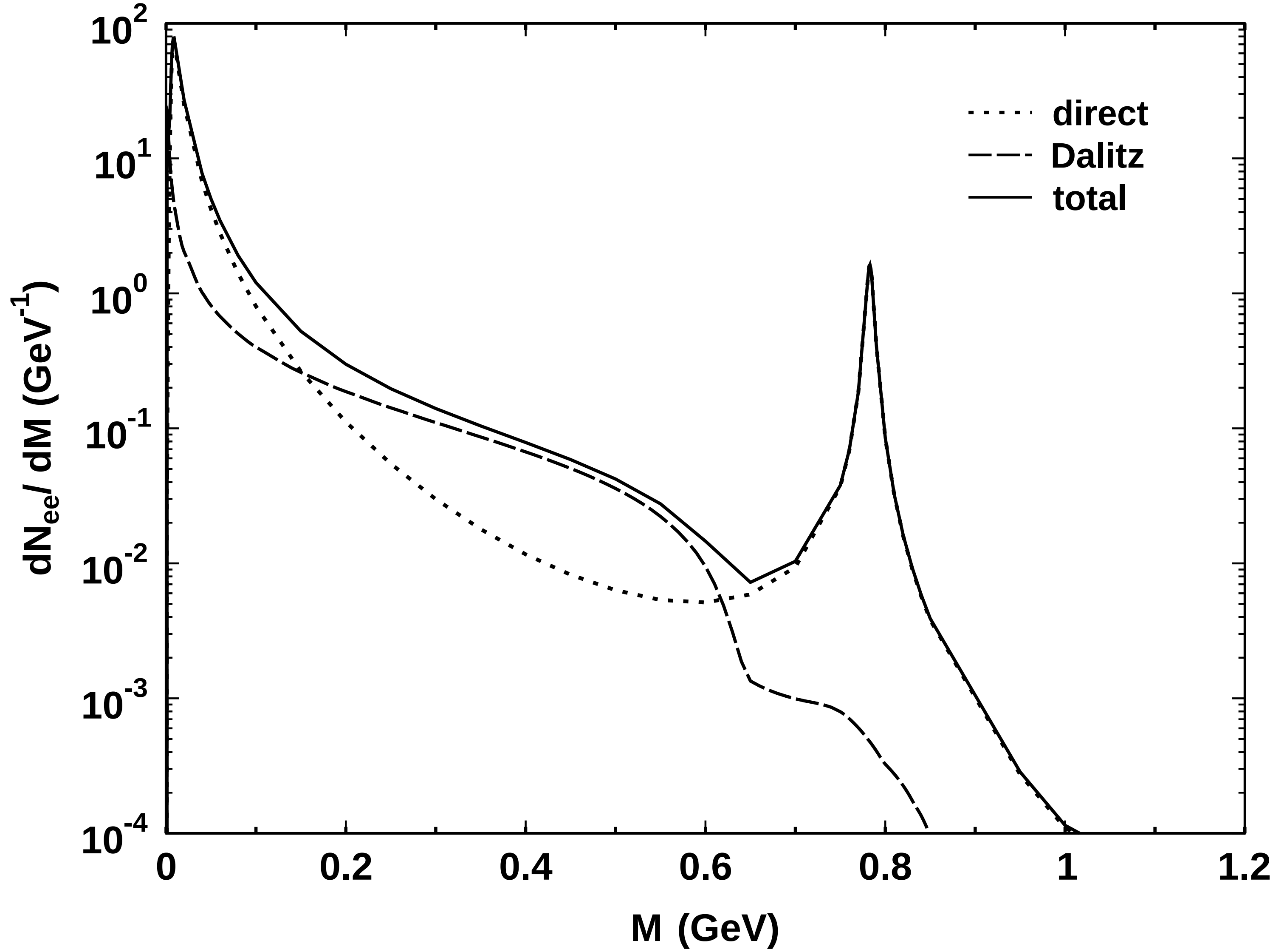

direct
Dalitz
total
dNee/ dM (GeV-1)
M (GeV)

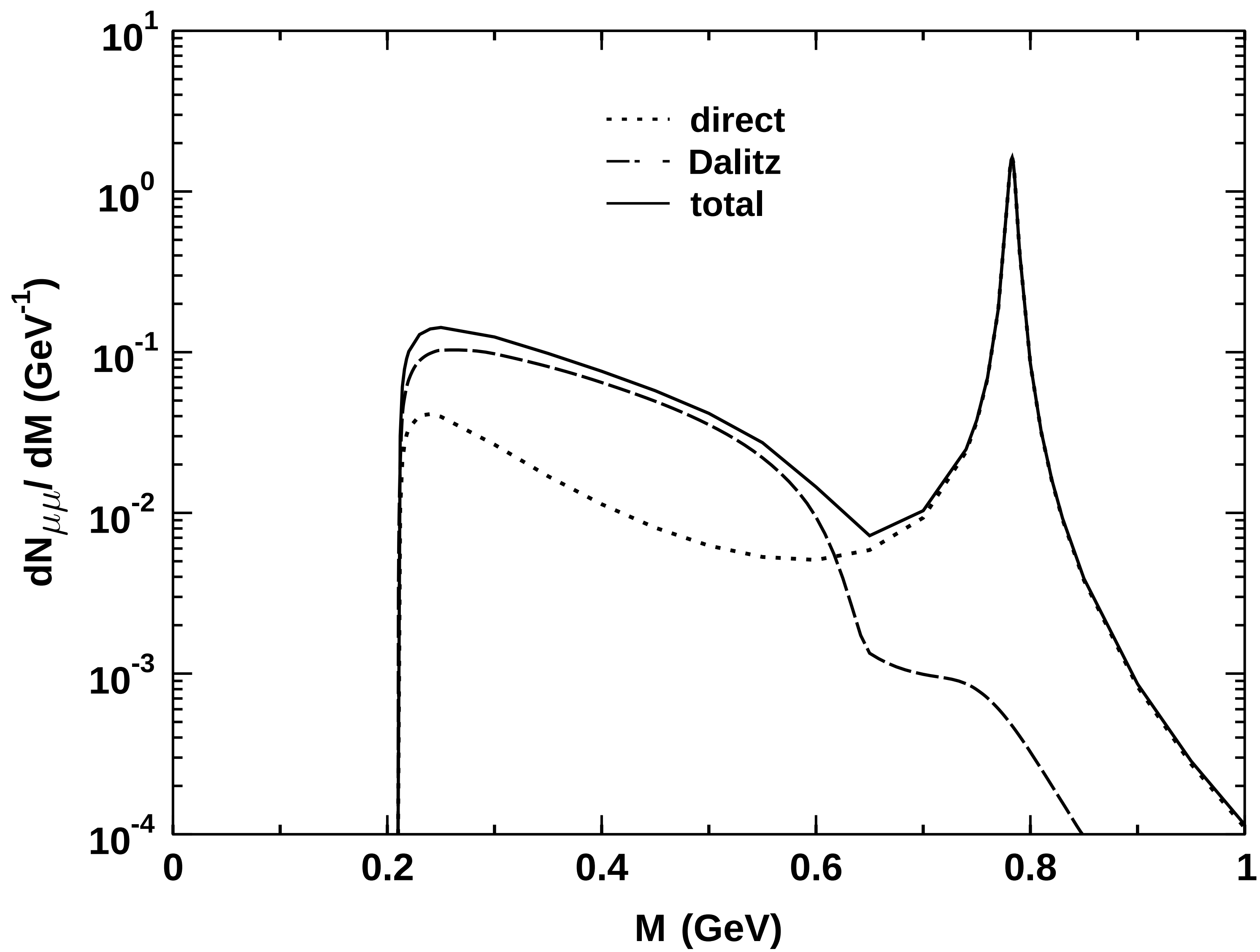

direct
Dalitz
total
$dN_{\mu\mu}/dM$ (GeV^{-1})
M (GeV)
10^{1}
10^{0}
10^{-1}
10^{-2}
10^{-3}
10^{-4}
0
0.2
0.4
0.6
0.8
1

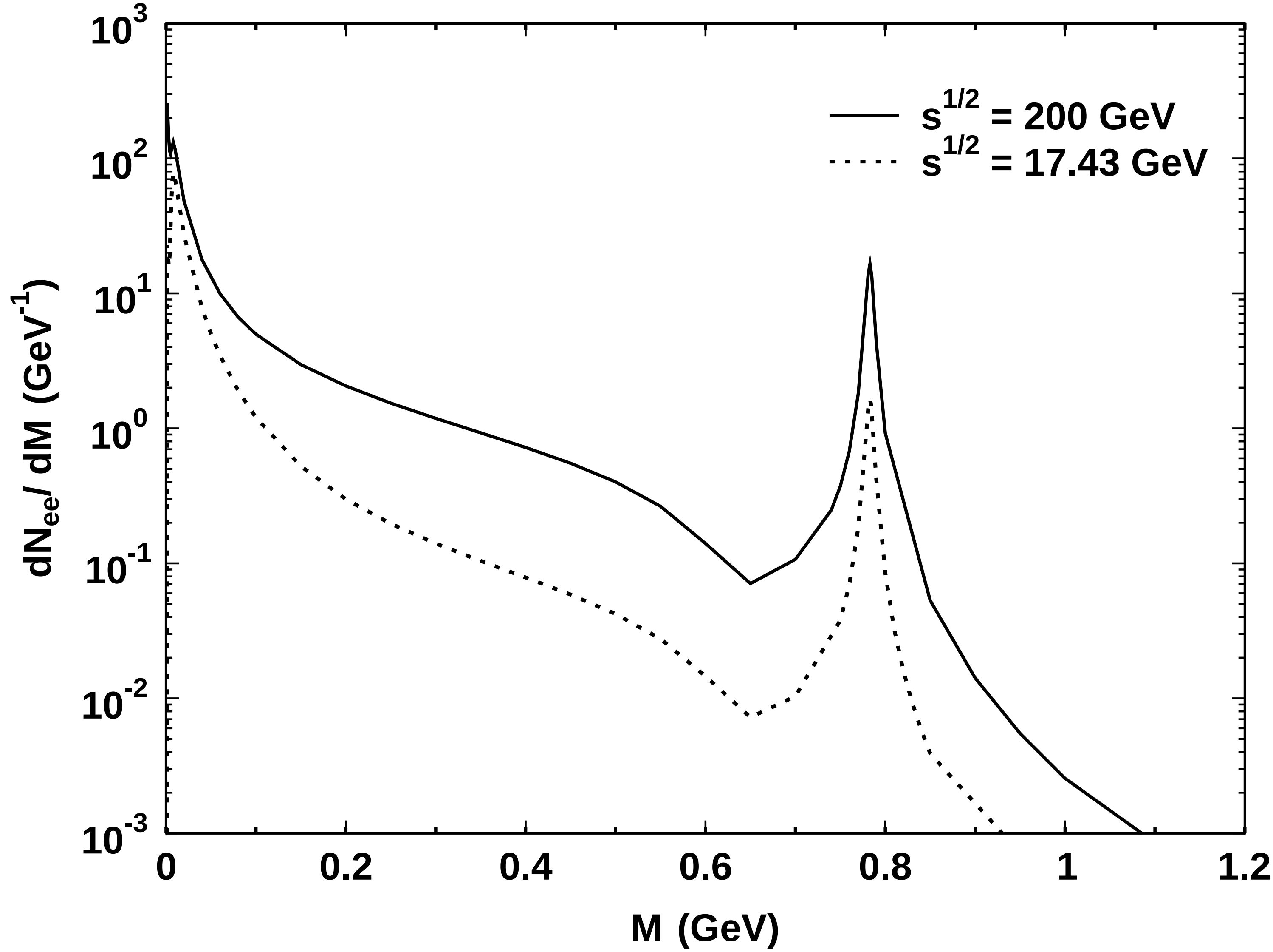
$s^{1/2}$ = 200 GeV
$s^{1/2}$ = 17.43 GeV
$dN_{ee}/\,dM$ (GeV^{-1})
M (GeV)
10^{3}
10^{2}
10^{1}
10^{0}
10^{-1}
10^{-2}
10^{-3}
0
0.2
0.4
0.6
0.8
1
1.2

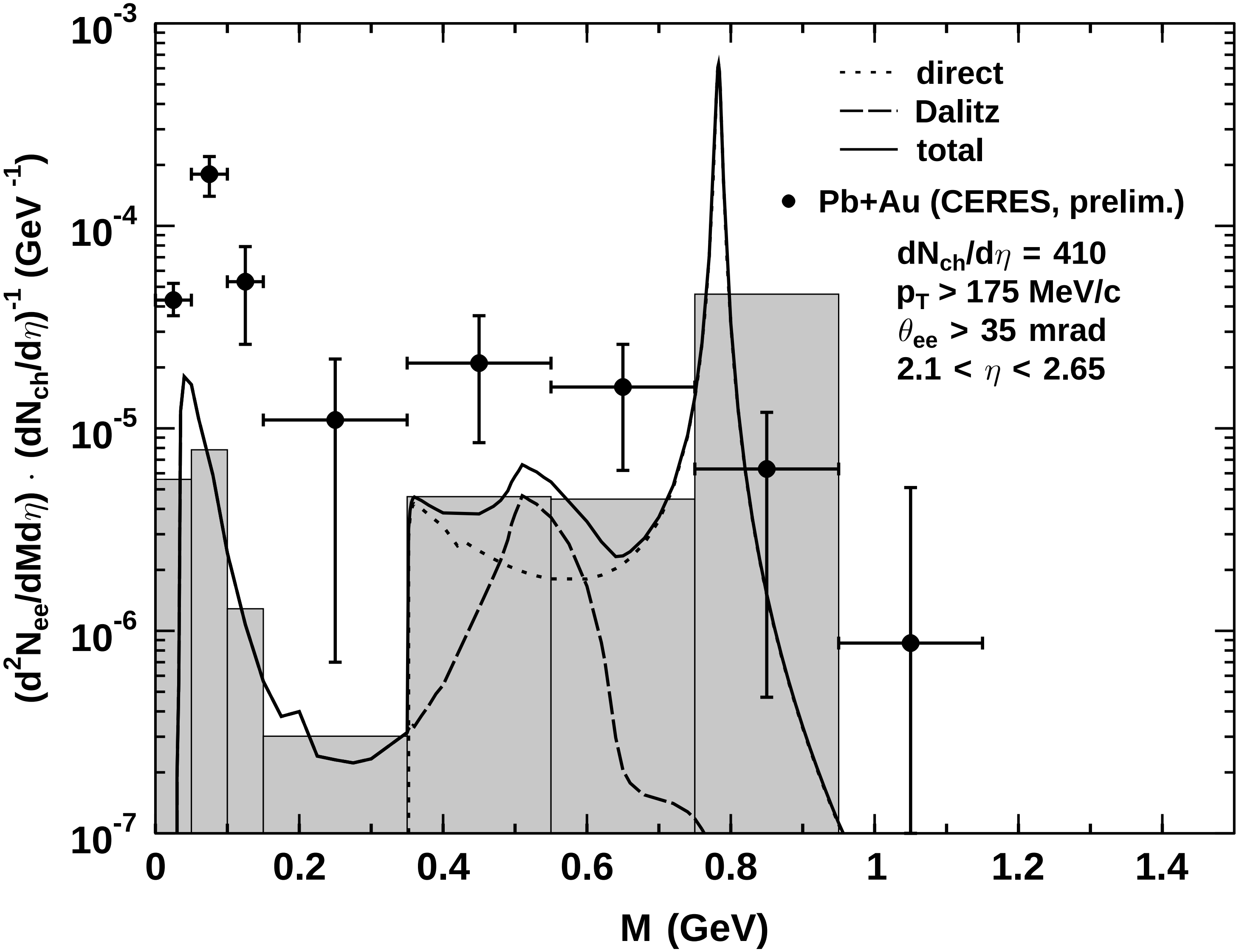
direct
Dalitz
total
Pb+Au (CERES, prelim.)
$dN_{ch}/d\eta$ = 410
p_T > 175 MeV/c
θ_{ee} > 35 mrad
2.1 < η < 2.65
$(d^2N_{ee}/dMd\eta) \cdot (dN_{ch}/d\eta)^{-1}$ (GeV $^{-1}$)
M (GeV)
10^{-3}
10^{-4}
10^{-5}
10^{-6}
10^{-7}
0
0.2
0.4
0.6
0.8
1
1.2
1.4

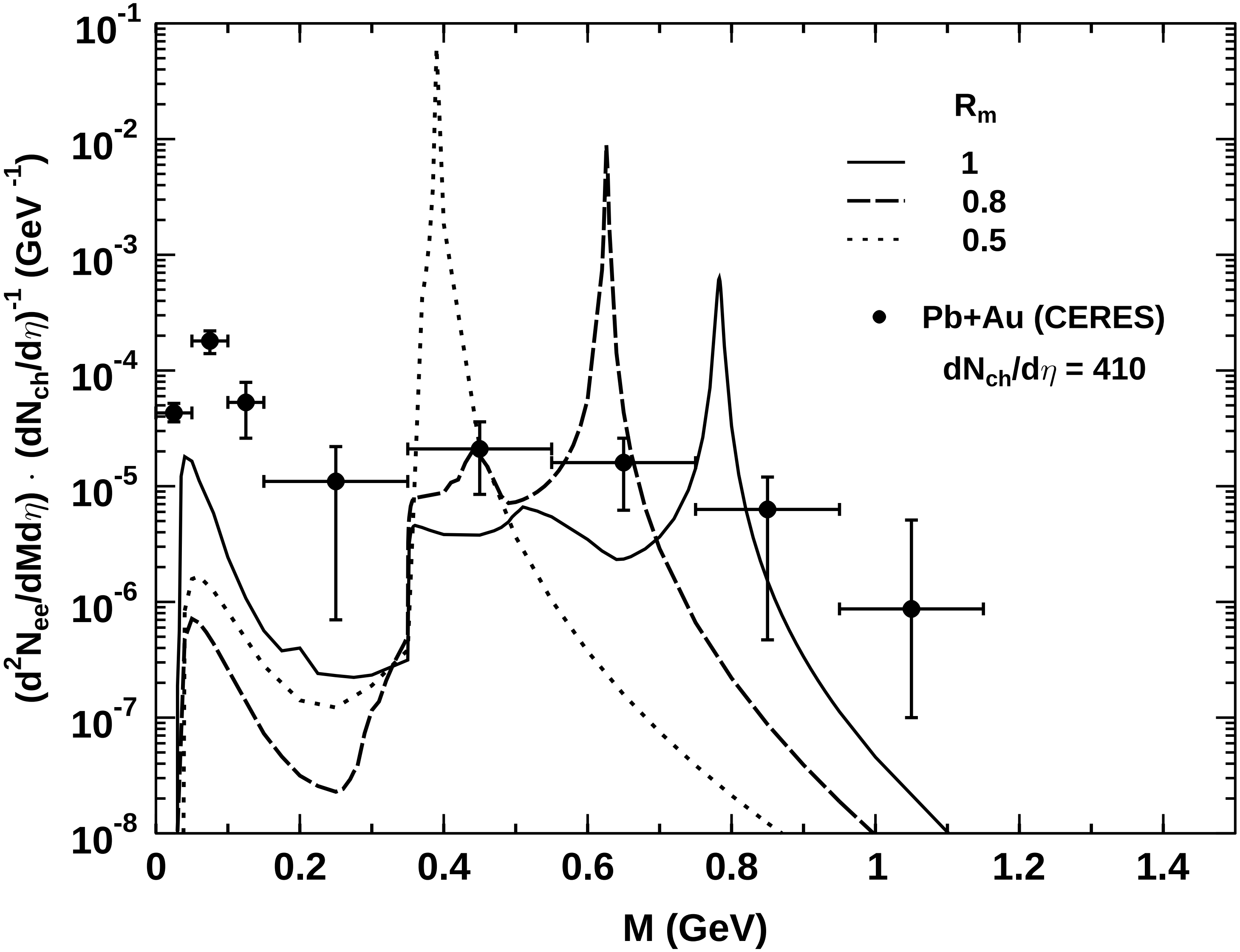

R_m
1
0.8
0.5
Pb+Au (CERES)
$dN_{ch}/d\eta = 410$
10^{-1}
10^{-2}
10^{-3}
10^{-4}
10^{-5}
10^{-6}
10^{-7}
10^{-8}
$(d^2N_{ee}/dMd\eta) \cdot (dN_{ch}/d\eta)^{-1}$ (GeV $^{-1}$)
0
0.2
0.4
0.6
0.8
1
1.2
1.4
M (GeV)

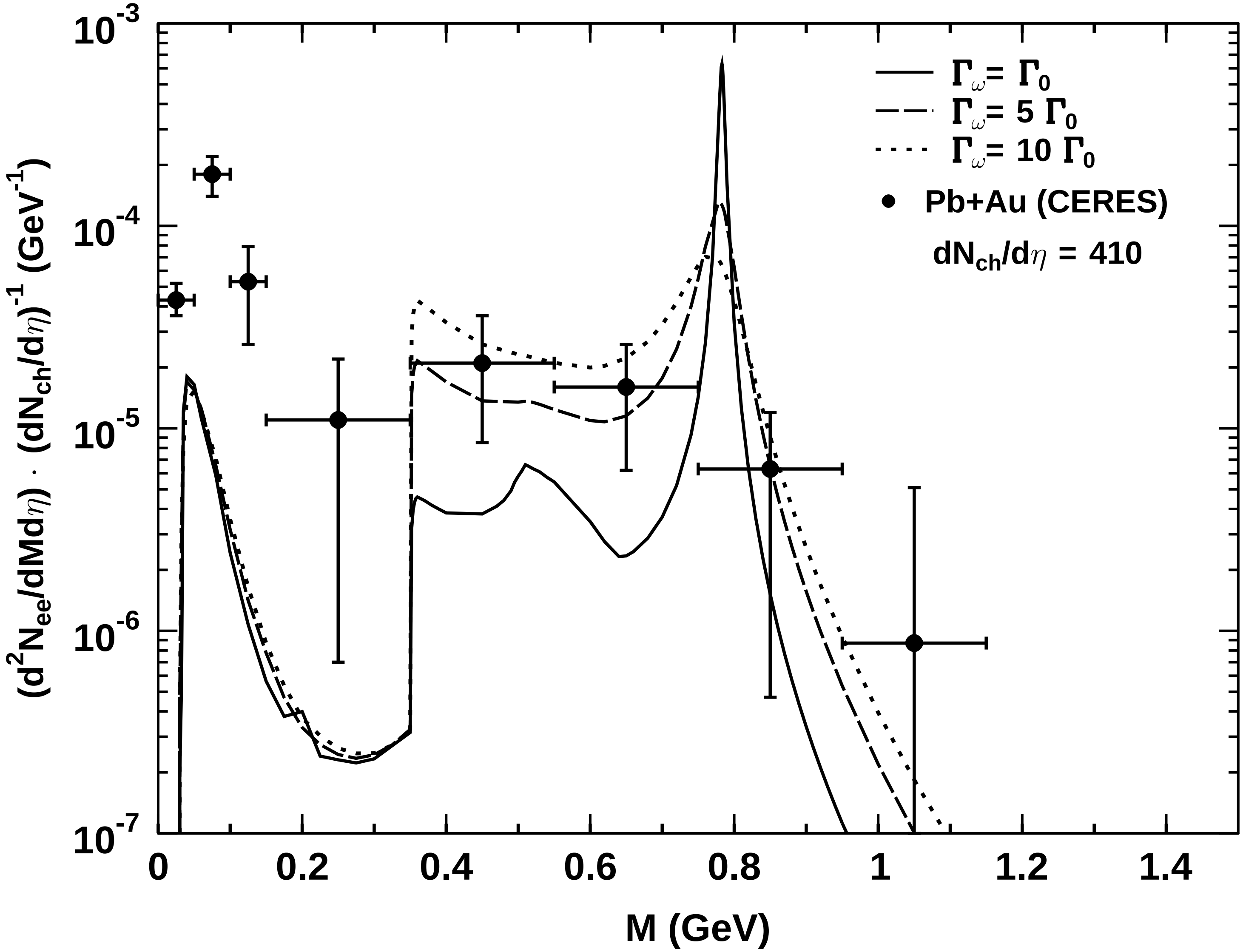

$\Gamma_\omega = \Gamma_0$
$\Gamma_\omega = 5\ \Gamma_0$
$\Gamma_\omega = 10\ \Gamma_0$
Pb+Au (CERES)
$dN_{ch}/d\eta = 410$
$(d^2N_{ee}/dMd\eta) \cdot (dN_{ch}/d\eta)^{-1}$ (GeV^{-1})
M (GeV)
10^{-3}
10^{-4}
10^{-5}
10^{-6}
10^{-7}
0
0.2
0.4
0.6
0.8
1
1.2
1.4